Design, synthesis and characterization of a urea-bridged periodic mesoporous organosilica supporting Cu nanoparticles (Cu@APS-TDU- PMO) as highly efficient and recoverable catalyst for the synthesis of tetrazole derivatives

Ehsan Valiey
Iran University of Science and Technology
Mohammad G. Dekamin (mdekamin@iust.ac.ir)
Iran University of Science and Technology

Article

Keywords: Urea-bridged periodic mesoporous organosilica (APS-TDU-PMO), Cu(II) supported on urea-bridged PMOs (Cu@APS-TDU-PMO), Tetrazole derivatives, Green Chemistry

Posted Date: April 12th, 2022

DOI: https://doi.org/10.21203/rs.3.rs-1528468/v1

Abstract

In this work, a new mesoporous periodic organosilica is introduced with urea-bridges obtained by the reaction of amino group of (3-aminopropyl) triethoxysilane and 2,4-toluene diisocyanate (APS-TDU-PMO). The obtained PMO-APS-TDU was found to be an appropriate support for loading of Cu(II) nanoparticles to afford Cu@APS-TDU-PMO. Uniformity and mesoporosity of both synthesized nanomaterials including PMO-APS-TDU and Cu@PMO-APS-TDU were characterized by different techniques such as FTIR, EDX, TGA, XRD, FESEM, BET, and TEM. Furthermore, the prepared Cu@APS-TDU-PMO was also used, as a heterogeneous and recyclable catalyst, for the synthesis of tetrazole derivatives through cascade condensation, concerted cycloaddition and tautomerization reactions. Indeed, the main advantages of this Cu@APS-TDU-PMO is its simple preparation and high catalytic activity as well as proper surface area which enable it to work under solvent-free conditions. Also, the introduced Cu@APS-TDU-PMO heterogeneous catalyst showed good stability and reusability for five consecutive runs to address more green chemistry principles.

Introduction

Mesoporous silica nanomaterials are widely used in materials science for various applications and as special blocks for making various valuable materials. Mesoporous silica nanomaterials have been extensively studied and used for various applications including catalysis, ion exchange, adsorption, molecular sieving, and even as templates for synthetic conductive carbon nanowires [1–20] due to their special properties such as large specific surface, high pore volume, uniform and tunable pores, high stability, and low cost [21–28]. Significant research efforts in recent years have been devoted to the development of periodic mesoporous organosilica (PMO) for applications in diverse fields. PMOs were first reported in 1999 [29–38]. PMOs are hybrid porous materials with high surface area and large porosity obtained by sol-gel method from an organo-bridged alkoxysilane in the presence of a surfactant [39–44]. The porous framework of PMOs is created by organic functional groups covalently binding to siloxane domains. In contrary to SBA-15 and MCM-41 which can only be functionalized at the surface by grafting methods, [45,46] different organic functionalities of organic-bridged silica precursor can be included in the silica framework [47–49]. PMOs have some advantages over periodic mesoporous silica (PMS) materials including mechanical stability, hydrophobic pore wall, and high concentration of organic functional group in the framework, which have led to applications in different fields such as hydrophobic drug carriers, [50] adsorbents, [51,52] biological/biomedical supports, [53]optical applications [54] solid chromatographic phases [55] and catalysis. [56–61] It is essential to use suitable catalytic systems for the preparation medically and ecologically very important compounds. Therefore, catalytic systems can be used for these purposes. The catalytic system consists of homogeneous and heterogeneous types. Also, heterogeneous catalysts have received more attention due to their many advantages such as easy separation from the reaction mixture, recyclability and less contamination in the final product. Among the various metal nanoparticles, copper nanoparticles are of particular importance due to their high conductivity, easy access, low cost, and tremendous copper potential to replace precious metals such as platinum,

gold, and silver. Immobilization of copper(II) on organic and inorganic ligands is one of the best methods for the production of heterogeneous catalysts with high stability, high activity and high load. Due to the use of copper complexes in various chemical reactions, such as the hydroboration reactions, [62,63] direct addition of terminal alkynes to imines, [64,65] alkyne-azide cycloaddition, [66] allylic alkylation reactions [67] and β-boration of α,β-unsaturated esters, [68] special attention has been paid to copper complexes as catalysts for these reactions. The catalytic synthesis of heterocyclic compounds, such as tetrazole derivatives, has received much attention in recent times [69–72]. Tetrazole derivatives are an important class of nitrogen-rich heterocyclic nucleus with widespread use as potential drug nuclei and compounds such as Lasortan, Irbesartan, and Tomelukast which have been developed into drugs [73–80]. In addition, application of tetrazole derivatives as important compounds in synthetic organic chemistry, [81,82] catalysis and energetic applications,[83] materials chemistry, [84] and as ligands in coordination chemistry [85] have led to the development of various efficient synthesis methods. Tetrazole derivatives are most commonly synthesized by [3 + 2] cycloaddition method [86–93]. Also, attempts for the production of tetrazole derivatives through new methods have led to the use of 2-benzylidenemalononitrile and sodium azide. This paper reports the synthesis of novel periodic mesoporous organosilica prepared by the reaction of amino group of (3-aminopropyl) triethoxysilane and 2,4-toluene diisocyanate (APS-TDU-PMO) with walls having urea bridges for Cu nanoparticles loading (Cu@APS-TDU-PMO, **1**). Also, the synthesized PMO was used as a highly efficient and recoverable catalyst for the synthesis of tetrazole derivatives via three-component addition of aldehydes, malononitrile, and sodium azide (Scheme 1).

Results And Discussion

The prepared Cu@APS-TDU-PMO (**1**) was characterized by FTIR, TEM, SEM, XRD, BET, EDX and TGA techniques.

FTIR spectrum of the synthesized PMO and Cu@APS-TDU-PMO (**1**) are shown in **Fig. 1**. The absorption band at 3414 cm^{-1} is attributed to N-H stretching. Two sharp absorption bands at 2928 cm^{-1} and 2862 cm^{-1} are assigned to the asymmetric and symmetric stretching of aliphatic C-H bonds, respectively. The absorption bands at 1682 cm^{-1} and 1654 cm^{-1} correspond to C=O bond stretching of the urea. The band at 1544 cm^{-1} can be assigned to the stretching vibration of the C=C bond. Two absorption bands at 1192 cm^{-1} and 1092 cm^{-1} are related to the Si-O-Si bonds (Fig. 1a). Also, the absorption band of Cu is clearly observed at 700-800 cm^{-1} (**Fig. 1b**).

Thermal gravimetric analysis (TGA) curve (**Fig. 2**) shows that the weight loss slightly below 100 °C can be assigned to the elimination of adsorbed surface water. Weight loss between 200-300 °C is due to the degradation of small amounts of the unextracted surfactant (P123). Also, weight loss between 300-600 °C is attributed to the removal of the bridge from the Cu@APS-TDU-PMO (**1**) structure.

FESEM and TEM images show that the Cu@APS-TDU-PMO (**1**) is composed of a large number of interwoven rods with 40.54-59.13 nm in width. It can also be seen that the morphology of PMO was

mostly preserved after deposition of Cu nanoparticles (**Fig. 3**). TEM images also demonstrate the honeycomb arrangement of mesopores and tubular mesochannels in the Cu@APS-TDU-PMO (**1**) structure, confirming the formation of a hexagonal mesoporous structure.

There is a peak at 2θ=1.35° in the low-angle XRD pattern, indicating the mesoporous structure of Cu@APS-TDU-PMO (**1**, **Fig. 4a**). Also, the wide-angle diffraction signal at 2θ of 20-30°, which is characteristic of mesoporous structures, is observed in the wide-angle XRD pattern of Cu@APS-TDU-PMO (**1**, **Fig. 4b**). The diffraction peaks at 2θ of 44.30°, 50.30°, and 75° can be assigned to the reflections of Cu (marked with ●).

EDX analysis confirms the presence of C, N, O, Si, and Cu elements in the Cu@APS-TDU-PMO (**1**) structure (**Fig. 5**).

The N_2 adsorption-desorption isotherm for Cu@APS-TDU-PMO (**1**) represents type IV isotherm commonly observed for mesoporous silica structures (**Fig. 6**). The calculated BET surface area was approximately 276 m^2 g^{-1} which was retained even after the deposition of Cu nanoparticles. The average pore size was about 5.74 nm (**Table 1**).

Table 1 Structural parameters of the Cu@APS-TDU-PMO (**1**) determined from nitrogen sorption experiments.

Sample	Pore diameter (nm)	Surface area (m^2 g^{-1})	Vp (cm^3 g^{-1})
Cu@APS-TDU-PMO (**1**)	5.74	276	0.17

Catalytic application of the Cu@APS-TDU-PMO (1) for the synthesis of 2-(1*H*-Tetrazol-5-yl) acrylonitrile derivatives

The catalytic performance of the prepared Cu@APS-TDU-PMO (**1**) was investigated for the synthesis of 2-(1*H*-Tetrazol-5-yl) acrylonitrile derivatives. To determine theoptimal reaction conditions for the three components of aromatic aldehyde (**2**), malononitrile (**3**), and sodium azide (**4**), the reaction was conducted using different solvents, temperatures, and catalyst loadings. The optimized reaction conditions are shown in **Table 2**. Initially, the reaction was performed under different conditions without catalyst. The obtained data showed that the reaction efficiency was negligible after 120 min (**Entry 1-7**). Then, the reaction was performed in EtOH, DMF, and solvent-free in the presence of 50 mg of catalyst, which solvent-free condition was more efficient (**Entry 8-10**). The results showed that the optimum amount of catalyst is 30 mg for the reaction, and a lower amount of catalysts leads to reduced efficiency of the reaction (**Entry 11-13**). Therefore, 30 mg of the catalyst in solvent-free conditions at 110 °C was selected as the optimal reaction condition for the synthesis of 2-(1*H*-Tetrazol-5-yl) acrylonitrile derivatives.

Table 2 Optimal condition for synthesis of 2-(1*H*-Tetrazol-5-yl) acrylonitrile derivatives[a] (**5a-i**).

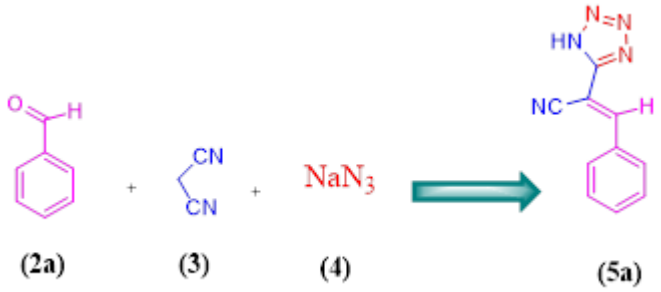

Entry	Catalyst	Catalyst loading (mg)	Solvent	Temperature (°C)	Time (h)	yield of (%) 5a
1	-	-	Solvent-Free	r.t.	120	Trace
2	-	-	H_2O	r.t.	120	Trace
3	-	-	DMF	r.t.	120	30
4	-	-	EtOH	r.t.	120	20
5	-	-	EtOH	Reflux	120	20
6	-	-	DMF	Reflux	120	40
7	-	-	Solvent-Free	110	120	45
8	Cu@APS-TDU-PMO (**1**)	50	EtOH	Reflux	50	38
9	Cu@APS-TDU-PMO (**1**)	50	DMF	Reflux	50	65
10	Cu@APS-TDU-PMO (**1**)	50	Solvent-Free	110	50	90
11	Cu@APS-TDU-PMO (**1**)	30	Solvent-Free	110	50	97
12	Cu@APS-TDU-PMO (**1**)	20	Solvent-Free	110	50	70
13	Cu@APS-TDU-PMO (**1**)	10	Solvent-Free	110	50	55

[a]Reaction conditions: aldehydes (**2a**, 1 mmol), malononitrile (**3**, 1 mmol), sodium azide (**4**, 1.2 mmol) and Cu@APS-TDU-PMO (**1**, 0.03 g) under different conditions.

Benzaldehyde with electron-withdrawing and electron-donating groups was used for the synthesis of 2-(1*H*- Tetrazol-5-yl) acrylonitrile derivatives, the results of which are summarized in **Table 3.**

Table 3 Scope of the 2-(1*H*-Tetrazol-5-yl) acrylonitrile derivatives catalysed using Cu@APS-TDU-PMO (**1**)[a].

Entry	Substrate (2)	product	Time (min)	Yield (%)
1	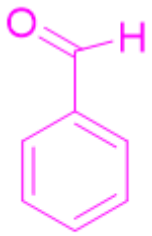 (2a)	 (5a)	50	97
2	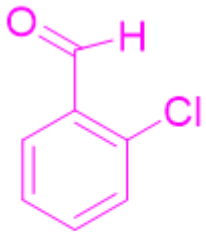 (2b)	 (5b)	52	93
3	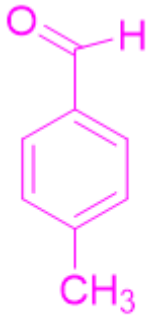 (2c)	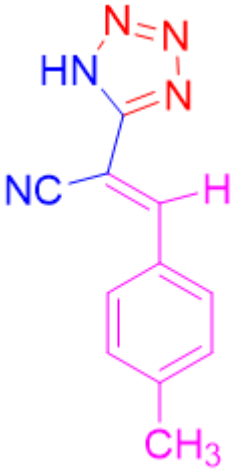 (5c)	55	92
4			60	89

	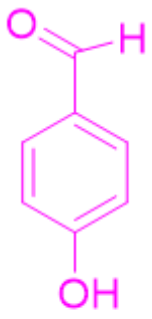 (2d)	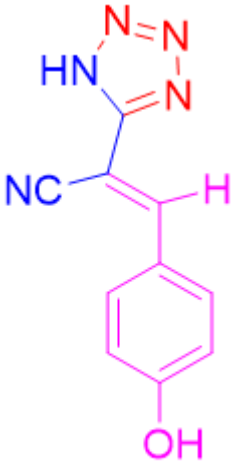 (5d)		
5	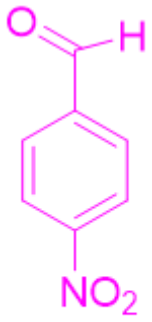 (2e)	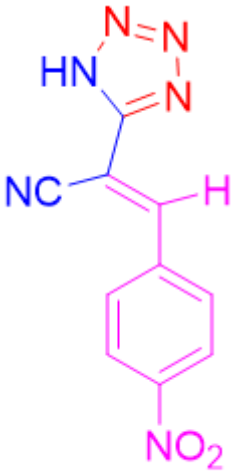 (5e)	60	91
6	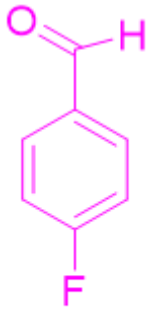 (2f)	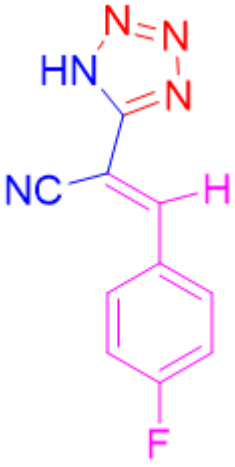 (5f)	56	93
7			53	92

	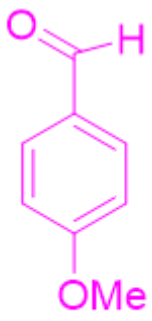 (2g)	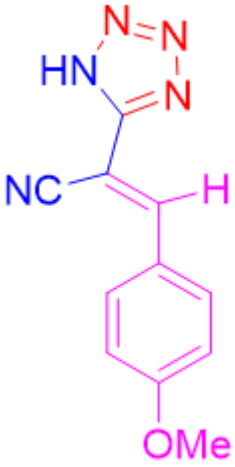 (5g)		
8	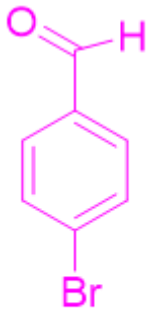 (2h)	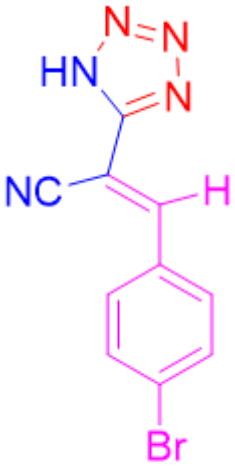 (5h)	56	89
9	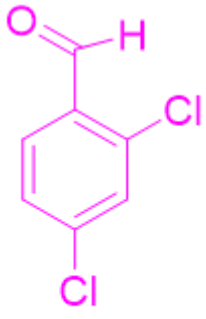 (2i)	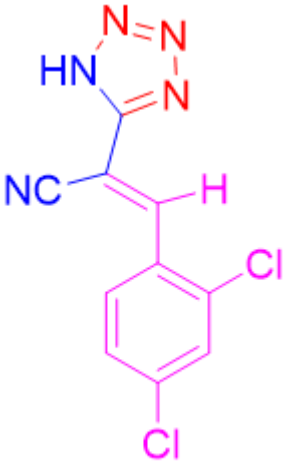 (5i)	52	92

[a]Reaction conditions: aldehydes (**2a**, 1 mmol), malononitrile (**3**, 1 mmol), sodium azide (**4**, 1.2 mmol) and Cu@APS-TDU-PMO (**1**, 0.03 g) under different conditions.

The proposed mechanism for the synthesis of 2-(1H-Tetrazol-5-yl) acrylonitrile derivatives

The proposed mechanism for the synthesis of 2-(1*H*-Tetrazol-5-yl) acrylonitrile derivatives is shown in **scheme 2**. Initially, the carbonyl group of aromatic aldehyde and the nitrile group of malononitrile are activated by the Cu@APS-TDU-PMO (**1**) catalyst. The Knoevenagel condensation reaction between the aromatic aldehyde and the malononitrile results in intermediate (**I**) formation. Then, Cu from the catalyst activates N of the intermediate (**I**), leading to [3+ 2] cycloaddition reaction between intermediate (**I**) and sodium azide. Subsequently, the catalyst was separated from intermediate (**II**) using an aqueous solution of HCl (acidic conditions) to obtain intermediate (**II**). Finally, 2-(1*H*-tetrazol-5-yl) acrylonitrile derivative as a more desirable tautomer was created via the tautomerization of intermediate (**II**).

Comparison of the catalytic activity of Cu@APS-TDU-PMO (1) catalyst

Table 4 compares the catalytic activity of Cu@APS-TDU-PMO (**1**) with other catalysts reported in the literature for the synthesis of 2-(1*H*-Tetrazol-5-yl) acrylonitrile derivatives. Specific properties of Cu@APS-TDU-PMO (**1**) catalyst, such as high efficiency, low catalyst loading, short reaction time, elimination of corrosive or expensive reagents, and reusability, make it superior to other reported catalysts.

Table 4 compares the catalytic activity of Cu@APS-TDU-PMO (**1**) with other catalysts reported.

Entry	Catalyst	Catalyst loading	Tempereture(°C)	Time (min)	References
1	Nano-NiO	0.06 mmol	70	360	94
2	Fe_3O_4@APTMS-DFX	0.03 g	120	60	95
3	Cu-MCM-41	0.03 g	140	720	96
4	Mesoporous ZnS	1 mmol	120	36 h	97
5	**Cu@APS-TDU-PMO (1)**	**0.03 g**	**110**	**30**	**This work**

Recyclability of Cu@APS-TDU-PMO (1)

Performing chemical reactions using recyclable and reusable catalysts is a significant issue in terms of green chemistry and environmental protection. In this study, recyclability of the catalyst was also investigated. For this purpose, the catalyst was separated from the reaction mixture using filtration, then washed with EtOH, and dried at 60 °C. The recycled catalyst was used in four consecutive reactions under optimal conditions for the synthesis of 2-(1*H*-Tetrazol-5-yl) acrylonitrile derivatives. As shown in **Fig. 7**, the catalytic activity of Cu@APS-TDU- PMO (**1**) was slightly decreased from 97 % to 85 %.

Experimental

Materials and Instrumentation

All chemicals were purchased from Merck or Aldrich. Characterization of the new Cu@APS-TDU-PMO (**1**) was performed by FESEM (TESCAN-MIRA3), TEM (Philips EM 208S), FTIR (Shimadzu 8400S), BET (ASAP

2020 micromeritics), and TGA Bahr Company STA 504). XRD patterns of the mesoporous silica nanosphere were obtained using TW 1800 diffractometer with Cu_{Ka} radiation (λ = 1.54050 Å). ^{1}H NMR (500 MHz, Bruker DRX-500 Avance spectrometers in DMSO) spectral were compared with those obtained from authentic samples or reported in the literature. Distilled water was used in all experiments.

General procedure for the preparation of 1,3-bis(3-(triethoxysilyl)propyl) urea bridge

First, (3-aminopropyl) triethoxysilane (APS, 6.52 mL) was added dropwise to 2,4-toluene diisocyanate (2 mL) and the mixture was stirred under solvent-free condition at 75 °C for 4 h. Then, the mixture was cooled down to room temperature and stirred for 12 h to obtain a white gel. Subsequently, $CHCl_3$ (10 mL) was added to the white gel and a clear solution was obtained, then hexane (10 mL) was added to it and a white precipitate was obtained which was separated by filtration and washed with hexane and dried at 70 °C.

General procedure for the preparation of PMO

P123 (4 g) as a surfactant was dissolved in 150 mL HCl (2M) and heated to 40 °C under stirring for 4 h. Then, the white powder (3.5 g) prepared above was dissolved in $CHCl_3$ and with TEOS (11.8 mL) added dropwise and simultaneously to the solution of P123 and HCl and stirred for 24 h at 40 °C and then aging for 48 h at 100 °C. Eventually, washed with EtOH (5 mL) and hexane (5 mL) and dried at 80 °C. The surfactant was extracted by a Soxhlet via EtOH-acidic. Finally, it was dried at 100 °C for 12 h.

General procedure for the preparation of Cu@APS-TDU-PMO (1)

$Cu(OAc)_2$ (0.5 g) was dissolved in 5 mL distilled water and this solution was added slowly to the suspension of PMO-APS-TDU (0.5 g) in 10 mL distilled water. The solution was stirred at room temperature for 24 h. Finally, the resulting solid was collected, washed with H_2O and EtOH, and dried at 60 °C for 5 h (**Scheme 3**).

General procedure for the preparation of 2-(1*H*-Tetrazol-5-yl) acrylonitrile derivatives

Cu@APS-TDU-PMO (**1**, 0.03 g), aromatic aldehyde (**2a-i**, 1 mmol), malononitrile (**3**, 1 mmol), and NaN_3 (**4**, 1.20 mmol) were heated to 110 °C under solvent-free conditions. The reaction development was monitored by TLC. After completion of the reaction, the reaction mixture dissolved in HCl (2M, 15 mL) and the catalyst was separated by filtration, then the resulting solution was extracted with EtOAc (3×10 mL). Finally, the solvent evaporated under reduced pressure and the desired product was recrystallized with EtOH-H_2O to afford the pure product. The recovered catalyst was reused for subsequent cycles without a loss of performance.

The FTIR, ^{1}HNMR and ^{13}CNMR data of tetrazole derivatives

3-(2-Chlorophenyl)-2-(1H-tetrazole-5-yl) acrylonitrile (**5b**)

FTIR (KBr, cm^{-1}): 3420 (NH), 2221 (CN), 1564 (C=C).; ^{1}HNMR (500MHz, $CDCl_3$): δ (ppm) 7.58–7.59 (2H, d, CH-Ar), 7.61–7.69 (1H, t, J= 7.20 Hz, CH-Ar), 8.13–8.14 (1H, d, CH-Ar), 8.54(1H, s, CH), 13.22 (br s, NH).; ^{13}CNMR (75 MHz, $CDCl_3$) δ (ppm) 80.14, 116.80, 129.17, 129.88, 130.73, 131.97, 134.39, 135.19, 147.04, 159.07, 161.37.

3-(4-Methoxyphenyl)-2-(1H-tetrazole-5-yl) acrylonitrile (**5g**)

FTIR (KBr, cm^{-1}): 31**46** (NH), 222**4** (CN), 15**86** (C=C).; ^{1}HNMR (500MHz, $CDCl_3$): δ (ppm) 3.82 (3H, s, OCH3), 7.09–7.11 (1H, d, CH-Ar), 7.96–7.99 (1H, d, CH-Ar), 8.21 (1H, s, CH), 13.70 (br s, NH). ^{13}CNMR (75 MHz, $CDCl_3$) δ (ppm) 56.02, 93.70, 115.25, 116.55, 125.21, 132.61, 147.97, 155.85, 162.91.

Conclusions

In conclusion, 2,5-toluenediisocyanate-based Cu@APS-TDU-PMO (**1**) with Cu nanoparticle loading was synthesized on the surface of pore wall. The synthesized Cu@APS-TDU-PMO (**1**) was characterized by using FTIR, EDX, TGA, XRD, FESEM, BET, and TEM techniques. It showed unique characteristics such as porous structure with adjustable pore size, high thermal stability, large surface area, and uniform pore size distribution. The synthesized Cu@APS-TDU-PMO (**1**) was efficiently used as a promising and recyclable catalyst for the synthesis of 2-(1*H*-Tetrazol-5-yl) acrylonitrile derivatives. In addition, the catalyst can be easily separated by filtration and used several times without significant reduction in catalytic activity. Other

Declarations

Availability of data and materials

The datasets generated and/or analysed during the current study would be available in the Science Data Bank repository after acceptance of the manuscript.

Acknowledgements

We are grateful for the financial support from The Research Council of Iran University of Science and Technology (IUST), Tehran, Iran (Grant No 160/20969) for their support. We would also like to acknowledge the support of The Iran Nanotechnology Initiative Council (INIC), Iran.

References

1. Corma, A. From microporous to mesoporous molecular sieve materials and their use in catalysis. Chemical reviews **97**, 2373–2420 (1997).
2. Sayari, A. & Hamoudi, S. Periodic mesoporous silica-based organic – inorganic nanocomposite materials. Chemistry of Materials **13**, 3151–3168 (2001).

3. Ying, J. Y., Mehnert, C. P. & Wong, M. S. Synthesis and applications of supramolecular-templated mesoporous materials. Angewandte Chemie International Edition **38**, 56–77 (1999).
4. Liu, X., Li, J., Zhou, L., Huang, D. & Zhou, Y. Adsorption of CO2, CH4 and N2 on ordered mesoporous silica molecular sieve. Chemical physics letters **415**, 198–201 (2005).
5. Grün, M., Kurganov, A., Schacht, S., Schüth, F. & Unger, K. Comparison of an ordered mesoporous aluminosilicate, silica, alumina, titania and zirconia in normal-phase high-performance liquid chromatography. Journal of Chromatography A **740**, 1–9 (1996).
6. Raja, R. & Thomas, J. M. Catalyst design strategies for controlling reactions in microporous and mesoporous molecular-sieves. Journal of Molecular Catalysis A: Chemical **181**, 3–14 (2002).
7. Jalili, F., Zarei, M., Zolfigol, M. A., Rostamnia, S. & Moosavi-Zare, A. R. SBA-15/PrN (CH2PO3H2) 2 as a novel and efficient mesoporous solid acid catalyst with phosphorous acid tags and its application on the synthesis of new pyrimido [4, 5-b] quinolones and pyrido [2, 3-d] pyrimidines via anomeric based oxidation. Microporous and Mesoporous Materials **294**, 109865 (2020).
8. Shaker, M. & Elhamifar, D. Magnetic methylene-based mesoporous organosilica composite-supported IL/Pd: a powerful and highly recoverable catalyst for oxidative coupling of phenols and naphthols. Materials Today Chemistry **18**, 100377 (2020).
9. dos Santos Andrade, L., Otubo, L., Castanheira, B. & Brochsztain, S. Novel periodic mesoporous organosilicas containing pyromellitimides and their application for the photodegradation of asphaltenes. Microporous and Mesoporous Materials **312**, 110740 (2021).
10. Zhao, W. *et al.* Light-responsive dual-functional biodegradable mesoporous silica nanoparticles with drug delivery and lubrication enhancement for the treatment of osteoarthritis. Nanoscale **13**, 6394–6399 (2021).
11. Liu, W. *et al.* Rational design of lanthanide nano periodic mesoporous organosilicas (Ln-nano-PMOs) for near-infrared emission. Dalton Transactions **50**, 2774–2781 (2021).
12. Castillo, X. *et al.* A cheap mesoporous silica from fly ash as an outstanding adsorbent for sulfate in water. Microporous and Mesoporous Materials **272**, 184–192 (2018).
13. Zhang, Z., Huang, Z. & Yuan, H. Direct conversion of cellulose to ethyl levulinate catalysed by modified fibrous mesoporous silica nanospheres in a co-solvent system. New Journal of Chemistry **45**, 5526–5539 (2021).
14. El-Sewify, I. M. & Khalil, M. M. Mesoporous nanosensors for sensitive monitoring and removal of copper ions in wastewater samples. New Journal of Chemistry **45**, 2573–2581 (2021).
15. Chatterjee, S. *et al.* Catalytic transformation of ethanol to methane and butene over NiO NPs supported over mesoporous SBA-15. Molecular Catalysis **502**, 111381 (2021).
16. Nikooei, N., Dekamin, M. G. & Valiey, E. Benzene-1,3,5-tricarboxylic acid-functionalized MCM-41 as a novel and recoverable hybrid catalyst for expeditious and efficient synthesis of 2,3-dihydroquinazolin-4(1H)-ones via one-pot three-component reaction. Research on Chemical Intermediates **46**, 3891–3909, doi:10.1007/s11164-020-04179-8 (2020).

17. Shendabadi, A. R. *et al.* 1, 3, 5-Tris (2-hydroxyethyl) Isocyanurate Functionalized SBA-15 (THEIC-SBA-15): as a Novel Heterogeneous Nano-Catalyst for the One-Pot Three-Component Synthesis of Tetrahydrobenzo b Pyrans in Water. *Biointerface Research in Applied Chemistry* **10**, 6706–6717 (2020).
18. Sam, M., Dekamin, M. G. & Alirezvani, Z. Dendrons containing boric acid and 1,3,5-tris(2-hydroxyethyl)isocyanurate covalently attached to silica-coated magnetite for the expeditious synthesis of Hantzsch esters. Scientific Reports **11**, 2399, doi:10.1038/s41598-020-80884-z (2021).
19. Cao, L. *et al.* Fluorophore-free luminescent double-shelled hollow mesoporous silica nanoparticles as pesticide delivery vehicles. Nanoscale **10**, 20354–20365 (2018).
20. Olivieri, F., Castaldo, R., Cocca, M., Gentile, G. & Lavorgna, M. Mesoporous silica nanoparticles as carriers of active agents for smart anticorrosive organic coatings: A critical review. Nanoscale **13**, 9091–9111 (2021).
21. Kumar, S., Malik, M. & Purohit, R. Synthesis methods of mesoporous silica materials. *Materials Today: Proceedings* **4**, 350–357 (2017).
22. Zebardasti, A., Dekamin, M. G. & Doustkhah, E. The Isocyanurate-Carbamate-Bridged Hybrid Mesoporous Organosilica: An Exceptional Anchor for Pd Nanoparticles and a Unique Catalyst for Nitroaromatics Reduction. Catalysts **11**, 621 (2021).
23. Amiri, A. A., Javanshir, S., Dolatkhah, Z. & Dekamin, M. G. SO 3 H-functionalized mesoporous silica materials as solid acid catalyst for facile and solvent-free synthesis of 2 H-indazolo [2, 1-b] phthalazine-1, 6, 11-trione derivatives. New Journal of Chemistry **39**, 9665–9671 (2015).
24. Cao, M. *et al.* New bi-functionalized ordered mesoporous material as heterogeneous catalyst for production of 5-hydroxymethylfurfural. Microporous and Mesoporous Materials **312**, 110709 (2021).
25. Valiey, E., Dekamin, M. G. & Alirezvani, Z. Sulfamic acid pyromellitic diamide-functionalized MCM-41 as a multifunctional hybrid catalyst for melting-assisted solvent-free synthesis of bioactive 3,4-dihydropyrimidin-2-(1H)-ones. Scientific Reports **11**, 11199, doi:10.1038/s41598-021-89572-y (2021).
26. Wei, Y. *et al.* Periodic mesoporous organosilica nanocubes with ultrahigh surface areas for efficient CO2 adsorption. Scientific reports **6**, 1–11 (2016).
27. Matsukawa, H. *et al.* Fast and stable vapochromic response induced through nanocrystal formation of a luminescent platinum (II) complex on periodic mesoporous organosilica. Scientific reports **9**, 1–11 (2019).
28. Mohanty, P. & Landskron, K. Periodic Mesoporous Organosilica Nanorice. Nanoscale Research Letters **4**, 169, doi:10.1007/s11671-008-9219-0 (2008).
29. Asefa, T., MacLachlan, M. J., Coombs, N. & Ozin, G. A. Periodic mesoporous organosilicas with organic groups inside the channel walls. Nature **402**, 867–871 (1999).
30. Inagaki, S., Guan, S., Fukushima, Y., Ohsuna, T. & Terasaki, O. Novel mesoporous materials with a uniform distribution of organic groups and inorganic oxide in their frameworks. Journal of the American Chemical Society **121**, 9611–9614 (1999).

31. Zebardasti, A., Dekamin, M. G., Doustkhah, E. & Assadi, M. H. N. Carbamate-Isocyanurate-Bridged Periodic Mesoporous Organosilica for van der Waals CO2 Capture. Inorganic Chemistry **59**, 11223–11227 (2020).
32. Akbari, A., Dekamin, M. G., Yaghoubi, A. & Naimi-Jamal, M. R. Novel magnetic propylsulfonic acid-anchored isocyanurate-based periodic mesoporous organosilica (Iron oxide@ PMO-ICS-PrSO 3 H) as a highly efficient and reusable nanoreactor for the sustainable synthesis of imidazopyrimidine derivatives. Scientific Reports **10**, 1–16 (2020).
33. Dekamin, M. G., Arefi, E. & Yaghoubi, A. Isocyanurate-based periodic mesoporous organosilica (PMO-ICS): a highly efficient and recoverable nanocatalyst for the one-pot synthesis of substituted imidazoles and benzimidazoles. RSC advances **6**, 86982–86988 (2016).
34. Li, P. *et al.* Selective Oxidation of Benzylic C–H Bonds Catalyzed by Cu (II)/{PMo12}. The Journal of organic chemistry **85**, 3101–3109 (2020).
35. Lin, X.-T. *et al.* Immobilized Zn (OAc) 2 on bipyridine-based periodic mesoporous organosilica for N-formylation of amines with CO 2 and hydrosilanes. New Journal of Chemistry **45**, 9501–9505 (2021).
36. Rajabi, F., Karimi, N., Luque, R. & Voskressensky, L. Highly ordered mesoporous functionalized pyridinium protic ionic liquid framework as a highly efficient catalytic system in chemoselective thioacetalization of carbonyl compounds under solvent-free conditions. Molecular Catalysis **515**, 111919 (2021).
37. Doustkhah, E. *et al.* Merging periodic mesoporous organosilica (PMO) with mesoporous aluminosilica (Al/Si-PMO): A catalyst for green oxidation. Molecular Catalysis **482**, 110676 (2020).
38. Akbari, A., Dekamin, M. G., Yaghoubi, A. & Naimi-Jamal, M. R. Novel magnetic propylsulfonic acid-anchored isocyanurate-based periodic mesoporous organosilica (Iron oxide@ PMO-ICS-PrSO3H) as a highly efficient and reusable nanoreactor for the sustainable synthesis of imidazopyrimidine derivatives. Scientific Reports **10**, 1–16 (2020).
39. Van Der Voort, P. *et al.* Periodic mesoporous organosilicas: from simple to complex bridges; a comprehensive overview of functions, morphologies and applications. Chemical Society Reviews **42**, 3913–3955 (2013).
40. Yaghoubi, A. & Dekamin, M. G. Green and Facile Synthesis of 4H-Pyran Scaffold Catalyzed by Pure Nano-Ordered Periodic Mesoporous Organosilica with Isocyanurate Framework (PMO-ICS). ChemistrySelect **2**, 9236–9243 (2017).
41. Yaghoubi, A., Dekamin, M. G. & Karimi, B. Propylsulfonic Acid-Anchored Isocyanurate-Based Periodic Mesoporous Organosilica (PMO-ICS-PrSO3H): A Highly Efficient and Recoverable Nanoporous Catalyst for the One-Pot Synthesis of Substituted Polyhydroquinolines. Catalysis Letters **147**, 2656–2663, doi:10.1007/s10562-017-2159-5 (2017).
42. Yaghoubi, A., Dekamin, M. G., Arefi, E. & Karimi, B. Propylsulfonic acid-anchored isocyanurate-based periodic mesoporous organosilica (PMO-ICS-Pr-SO3H): A new and highly efficient recoverable

nanoporous catalyst for the one-pot synthesis of bis (indolyl) methane derivatives. Journal of colloid and interface science **505**, 956–963 (2017).

43. Elhamifar, D., Nasr-Esfahani, M., Karimi, B., Moshkelgosha, R. & Shábani, A. Ionic liquid and sulfonic acid based bifunctional periodic mesoporous organosilica (BPMO–IL–SO3H) as a highly efficient and reusable nanocatalyst for the biginelli reaction. ChemCatChem **6**, 2593–2599 (2014).
44. Kaczmarek, A. M. *et al.* Amine-containing (nano-) Periodic Mesoporous Organosilica and its application in catalysis, sorption and luminescence. Microporous and Mesoporous Materials **291**, 109687 (2020).
45. Alirezvani, Z., Dekamin, M. G. & Valiey, E. New hydrogen-bond-enriched 1, 3, 5-tris (2-hydroxyethyl) isocyanurate covalently functionalized MCM-41: an efficient and recoverable hybrid catalyst for convenient synthesis of acridinedione derivatives. ACS omega **4**, 20618–20633 (2019).
46. Eslami, M., Dekamin, M. G., Motlagh, L. & Maleki, A. MCM-41 mesoporous silica: a highly efficient and recoverable catalyst for rapid synthesis of α-aminonitriles and imines. Green Chemistry Letters and Reviews **11**, 36–46 (2018).
47. Kresge, C. T., Leonowicz, M. E., Roth, W. J., Vartuli, J. C. & Beck, J. S. Ordered mesoporous molecular sieves synthesized by a liquid-crystal template mechanism. *nature* **359**, 710–712 (1992).
48. Zhao, D. *et al.* Triblock copolymer syntheses of mesoporous silica with periodic 50 to 300 angstrom pores. *science* **279**, 548–552 (1998).
49. Mashayekhi, S. *et al.* Curcumin-loaded mesoporous silica nanoparticles/nanofiber composites for supporting long-term proliferation and stemness preservation of adipose-derived stem cells. International journal of pharmaceutics **587**, 119656 (2020).
50. Teng, Z. *et al.* Facile Synthesis of Yolk–Shell-Structured Triple-Hybridized Periodic Mesoporous Organosilica Nanoparticles for Biomedicine. Small **12**, 3550–3558 (2016).
51. Sim, K. *et al.* CO2 adsorption on amine-functionalized periodic mesoporous benzenesilicas. ACS applied materials & interfaces **7**, 6792–6802 (2015).
52. De Canck, E., Ascoop, I., Sayari, A. & Van Der Voort, P. Periodic mesoporous organosilicas functionalized with a wide variety of amines for CO 2 adsorption. Physical Chemistry Chemical Physics **15**, 9792–9799 (2013).
53. De Canck, E., Esquivel, D., Romero-Salguero, F. J. & Van Der Voort, P. Periodic mesoporous organosilicas: hybrid porous materials with exciting applications. COMPREHENSIVE GUIDE FOR MESOPOROUS MATERIALS, 197 (2015).
54. Kaczmarek, A. M. & Van Der Voort, P. Light-emitting lanthanide periodic mesoporous organosilica (PMO) hybrid materials. Materials **13**, 566 (2020).
55. Wu, C. *et al.* Clickable periodic mesoporous organosilica monolith for highly efficient capillary chromatographic separation. Analytical chemistry **88**, 1521–1525 (2016).
56. Ha, C.-S. & Park, S. S. in *Periodic Mesoporous Organosilicas: Preparation, Properties and Applications* (eds Chang-Sik Ha & Sung Soo Park) 125–187 (Springer Singapore, 2019).

57. Karimi, B., Ganji, N., Pourshiani, O. & Thiel, W. R. Periodic mesoporous organosilicas (PMOs): From synthesis strategies to applications. Progress in Materials Science **125**, 100896, doi:https://doi.org/10.1016/j.pmatsci.2021.100896 (2022).
58. Liu, J. *et al.* Yolk–shell hybrid materials with a periodic mesoporous organosilica shell: ideal nanoreactors for selective alcohol oxidation. Advanced Functional Materials **22**, 591–599 (2012).
59. Liu, X., Maegawa, Y., Goto, Y., Hara, K. & Inagaki, S. Heterogeneous catalysis for water oxidation by an iridium complex immobilized on bipyridine-periodic mesoporous organosilica. Angewandte Chemie International Edition **55**, 7943–7947 (2016).
60. Valiey, E. & Dekamin, M. G. Pyromellitic diamide–diacid bridged mesoporous organosilica nanospheres with controllable morphologies: a novel PMO for the facile and expeditious synthesis of imidazole derivatives. Nanoscale Advances **4**, 294–308, doi:10.1039/D1NA00738F (2022).
61. Valiey, E. & Dekamin, M. G. Supported copper on a diamide–diacid-bridged PMO: an efficient hybrid catalyst for the cascade oxidation of benzyl alcohols/Knoevenagel condensation. RSC Advances **12**, 437–450, doi:10.1039/D1RA06509B (2022).
62. Lee, Y. & Hoveyda, A. H. Efficient boron – copper additions to aryl-substituted alkenes promoted by NHC – based catalysts. Enantioselective Cu-catalyzed hydroboration reactions. Journal of the American Chemical Society **131**, 3160–3161 (2009).
63. Ton, N. N., Mai, B. K. & Nguyen, T. V. Tropylium-Promoted Hydroboration Reactions: Mechanistic Insights Via Experimental and Computational Studies. The Journal of Organic Chemistry (2021).
64. Wei, C. & Li, C.-J. Enantioselective direct-addition of terminal alkynes to imines catalyzed by copper (I) pybox complex in water and in toluene. Journal of the American Chemical Society **124**, 5638–5639 (2002).
65. Shah, S., Das, B. G. & Singh, V. K. Recent advancement in copper-catalyzed asymmetric reactions of alkynes. Tetrahedron, 132238 (2021).
66. Ghanbari, Z. & Naeimi, H. Tetrazol-Cu (i) immobilized on nickel ferrite catalyzed green synthesis of indenopyridopyrimidine derivatives in aqueous media. RSC Advances **11**, 31377–31384 (2021).
67. Van Veldhuizen, J. J., Campbell, J. E., Giudici, R. E. & Hoveyda, A. H. A readily available chiral Ag-based N-heterocyclic carbene complex for use in efficient and highly enantioselective Ru-catalyzed olefin metathesis and Cu-catalyzed allylic alkylation reactions. Journal of the American Chemical Society **127**, 6877–6882 (2005).
68. Lillo, V. *et al.* Asymmetric β-boration of α, β-unsaturated esters with chiral (NHC) Cu catalysts. Organometallics **28**, 659–662 (2009).
69. Sharghi, H., Ebrahimpourmoghaddam, S. & Doroodmand, M. M. Facile synthesis of 5-substituted-1H-tetrazoles and 1-substituted-1H-tetrazoles catalyzed by recyclable 4'-phenyl-2, 2': 6', 2 "-terpyridine copper (II) complex immobilized onto activated multi-walled carbon nanotubes. Journal of organometallic chemistry **738**, 41–48 (2013).
70. Tourani, H., Naimi-Jamal, M. R., Panahi, L. & Dekamin, M. G. Nanoporous metal-organic framework Cu2 (BDC) 2 (DABCO) as an efficient heterogeneous catalyst for one-pot facile synthesis of 1, 2, 3-

triazole derivatives in ethanol: Evaluating antimicrobial activity of the novel derivatives. Scientia Iranica **26**, 1485–1496 (2019).

71. Tourani, H., Naimi-Jamal, M. R. & Dekamin, M. G. Preparation of 5-Substituted-1H-Tetrazoles Catalyzed by MOFs via Two Strategies: Direct Condensation of Aryl Nitriles with Sodium Azide, and Tri-Component Reaction Method. *ChemistrySelect* **3**, 8332–8337 (2018).
72. Sajjadifar, S., Zolfigol, M. A. & Chehardoli, G. Boron sulfuric acid as an efficient heterogeneous catalyst for the synthesis of 1-substituted 1H-1, 2, 3, 4-tetrazoles in polyethylene glycol. Eurasian Chemical Communications **2**, 812–818 (2020).
73. Patani, G. A. & LaVoie, E. J. Bioisosterism: a rational approach in drug design. Chemical reviews **96**, 3147–3176 (1996).
74. Ornstein, P. L. *et al.* Structure – activity studies of 6-(tetrazolylalkyl)-substituted decahydroisoquinoline-3-carboxylic acid AMPA receptor antagonists. 1. Effects of stereochemistry, chain length, and chain substitution. Journal of medicinal chemistry **39**, 2219–2231 (1996).
75. Kees, K. L., Cheeseman, R. S., Prozialeck, D. H. & Steiner, K. E. Perfluoro-N-[4-(1H-tetrazol-5-ylmethyl) phenyl] alkanamides. A new class of oral antidiabetic agents. Journal of medicinal chemistry **32**, 11–13 (1989).
76. Singh, H., Chawla, A. S., Kapoor, V. K., Paul, D. & Malhotra, R. K. 4 Medicinal chemistry of tetrazoles. Progress in medicinal chemistry **17**, 151–183 (1980).
77. Bary, V., Conalty, M., O'SIlivan, J. & Twomey, D. Chemother., Chemother. *Proc. 9th Int. Congr* **8**, 103 (1977).
78. Okabayashi, T. kano, H.; Makisumi. Y. Chem Pharm Bull **8**, 157 (1960).
79. Molaei, S., Tamoradi, T., Ghadermazi, M. & Ghorbani-Choghamarani, A. Synthesis and characterization of MCM-41@ AMPD@ Zn as a novel and recoverable mesostructured catalyst for oxidation of sulfur containing compounds and synthesis of 5-substituted tetrazoles. Microporous and Mesoporous Materials **272**, 241–250 (2018).
80. Prasad, A. N., Reddy, B. M., Jeong, E.-Y. & Park, S.-E. Cu (II) PBS-bridged PMOs catalyzed one-pot synthesis of 1, 4-disubstituted 1, 2, 3-triazoles in water through click chemistry. RSC Advances **4**, 29772–29781 (2014).
81. Jin, T., Kamijo, S. & Yamamoto, Y. Synthesis of 1-substituted tetrazoles via the acid-catalyzed [3 + 2] cycloaddition between isocyanides and trimethylsilyl azide. Tetrahedron letters **45**, 9435–9437 (2004).
82. Stierstorfer, J., Wurzenberger, M. H. H., Weippert, V. & Braun, V. Tailoring the properties of 3d transition metal complexes with different N-cycloalkyl-substituted tetrazoles. New Journal of Chemistry (2021).
83. Nasrollahzadeh, M., Nezafat, Z., Bidgoli, N. S. S. & Shafiei, N. Use of tetrazoles in catalysis and energetic applications: Recent developments. Molecular Catalysis **513**, 111788, doi:https://doi.org/10.1016/j.mcat.2021.111788 (2021).
84. Koguro, K., Oga, T., Mitsui, S. & Orita, R. Novel synthesis of 5-substituted tetrazoles from nitriles. *Synthesis* 1998, 910–914 (1998).

85. Sauer, J., Huisgen, R. & Sturm, H. Zur acylierung von 5-aryl-tetrazolen; ein duplikationsverfahren zur darstellung von polyarylen. Tetrahedron **11**, 241–251 (1960).
86. Swami, S., Sahu, S. N. & Shrivastava, R. Nanomaterial catalyzed green synthesis of tetrazoles and its derivatives: a review on recent advancements. RSC Advances **11**, 39058–39086, doi:10.1039/D1RA05955F (2021).
87. Heravi, M. M., Zadsirjan, V., Dehghani, M. & Ahmadi, T. Towards click chemistry: Multicomponent reactions via combinations of name reactions. Tetrahedron **74**, 3391–3457, doi:https://doi.org/10.1016/j.tet.2018.04.076 (2018).
88. El Anwar, S., Růžičková, Z., Bavol, D., Fojt, L. & Grüner, B. Tetrazole Ring Substitution at Carbon and Boron Sites of the Cobalt Bis(dicarbollide) Ion Available via Dipolar Cycloadditions. Inorganic Chemistry **59**, 17430–17442, doi:10.1021/acs.inorgchem.0c02719 (2020).
89. Mittal, R. & Awasthi, S. K. Recent Advances in the Synthesis of 5-Substituted 1H-Tetrazoles: A Complete Survey (2013–2018). Synthesis **51**, 3765–3783 (2019).
90. Shelkar, R., Singh, A. & Nagarkar, J. Amberlyst-15 catalyzed synthesis of 5-substituted 1-H-tetrazole via [3 + 2] cycloaddition of nitriles and sodium azide. Tetrahedron Letters **54**, 106–109, doi:https://doi.org/10.1016/j.tetlet.2012.10.116 (2013).
91. Yuan, X., Wang, Z., Zhang, Q. & Luo, J. An intramolecular relay catalysis strategy for Knoevenagel condensation and 1,3-dipolar cycloaddition domino reactions. RSC Advances **9**, 23614–23621, doi:10.1039/C9RA04081A (2019).
92. *Scientia Iranica* **26**, 1463–1473, doi:10.24200/sci.2018.21088 (2019).
93. Kamijo, S. *et al.* Tetrazole synthesis via the palladium-catalyzed three component coupling reaction. Molecular Diversity **6**, 181–192, doi:10.1023/B:MODI.0000006755.04495.d3 (2003).
94. Safaei-Ghomi, J. & Paymard-Samani, S. Facile and rapid synthesis of 5-substituted 1H-tetrazoles via a multicomponent domino reaction using nickel (II) oxide nanoparticles as catalyst. Chemistry of Heterocyclic Compounds **50**, 1567–1574 (2015).
95. Taghavi, F., Gholizadeh, M., Saljooghi, A. S. & Ramezani, M. Cu (ii) immobilized on Fe 3 O 4@ APTMS-DFX nanoparticles: an efficient catalyst for the synthesis of 5-substituted 1 H-tetrazoles with cytotoxic activity. MedChemComm **8**, 1953–1964 (2017).
96. Abdollahi-Alibeik, M. & Moaddeli, A. Multi-component one-pot reaction of aldehyde, hydroxylamine and sodium azide catalyzed by Cu-MCM-41 nanoparticles: a novel method for the synthesis of 5-substituted 1 H-tetrazole derivatives. New Journal of Chemistry **39**, 2116–2122 (2015).
97. Lang, L., Zhou, H., Xue, M., Wang, X. & Xu, Z. Mesoporous ZnS hollow spheres-catalyzed synthesis of 5-substituted 1H-tetrazoles. Materials Letters **106**, 443–446 (2013).

Schemes

Schemes 1, 2 and 3 are available in Supplementary Files section.

Figures

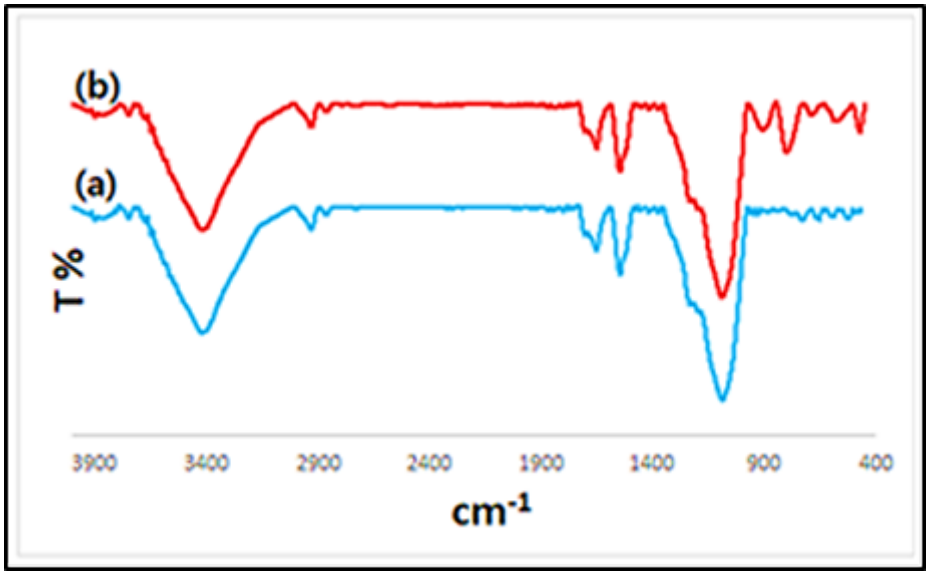

Figure 1

FTIR spectra of the PMO (**a**) and Cu@APS-TDU-PMO (**1**, **b**).

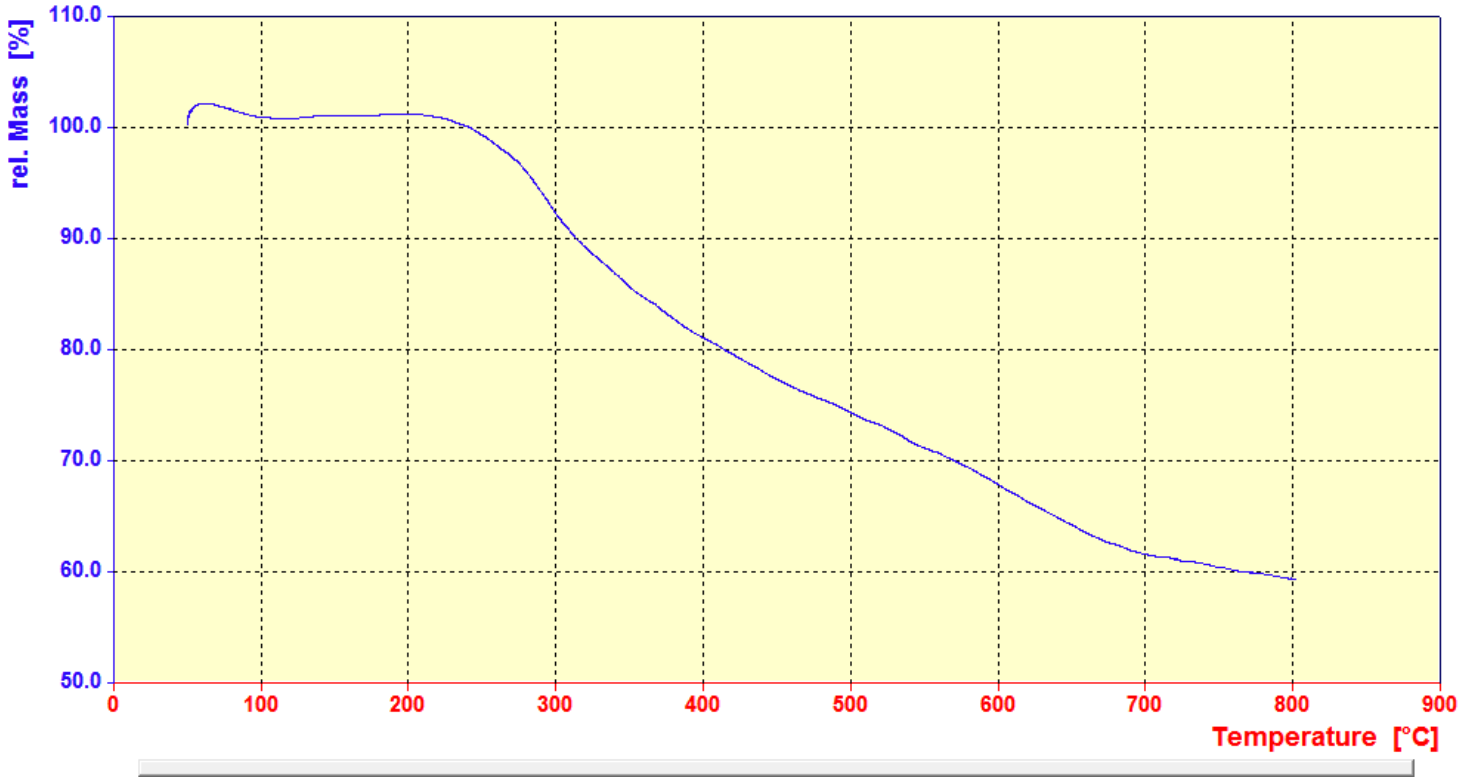

Figure 2

TGA of the Cu@APS-TDU-PMO (**1**).

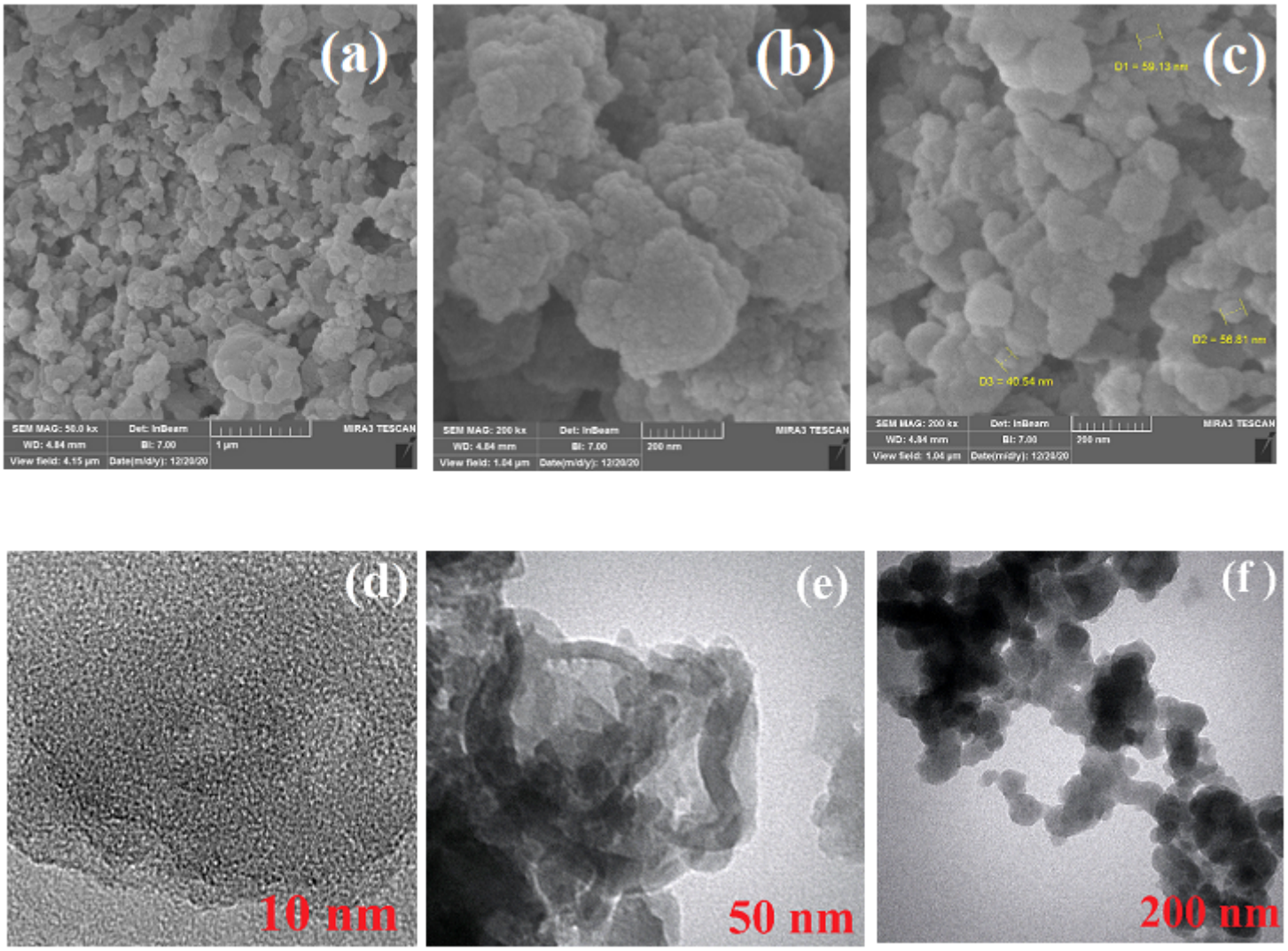

Figure 3

(**a**, **b**, **c**) SEM, and (**d**, **e**, **f**) TEM images of the Cu@APS-TDU-PMO (**1**).

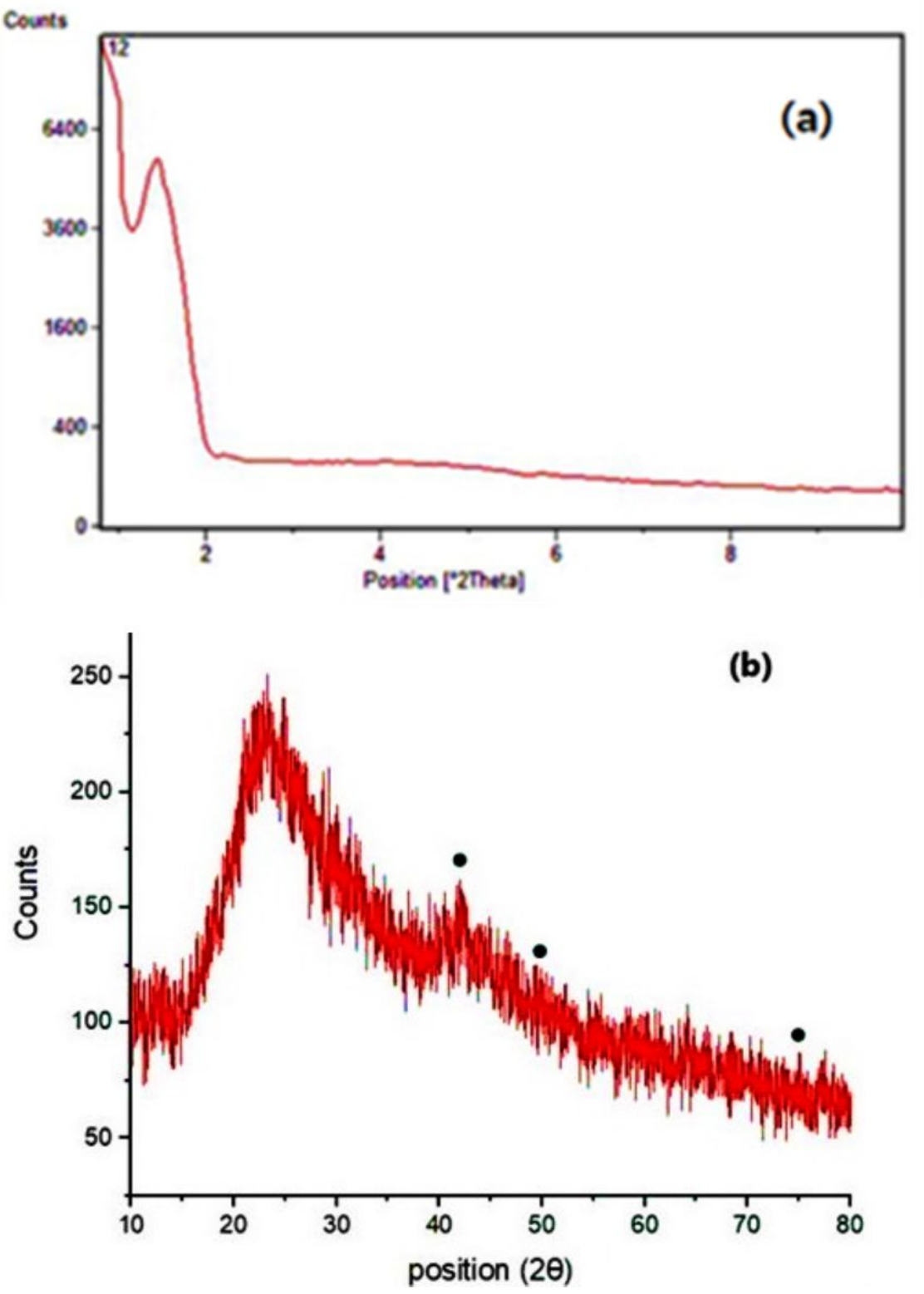

Figure 4

Low-angle (**a**) and wide angle (**b**) XRD patterns of the Cu@APS-TDU-PMO (**1**).

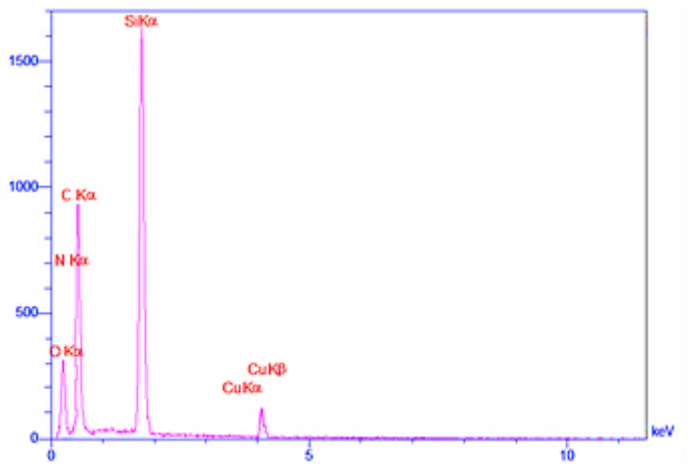

Figure 5

EDX analysis of the Cu@APS-TDU-PMO (**1**).

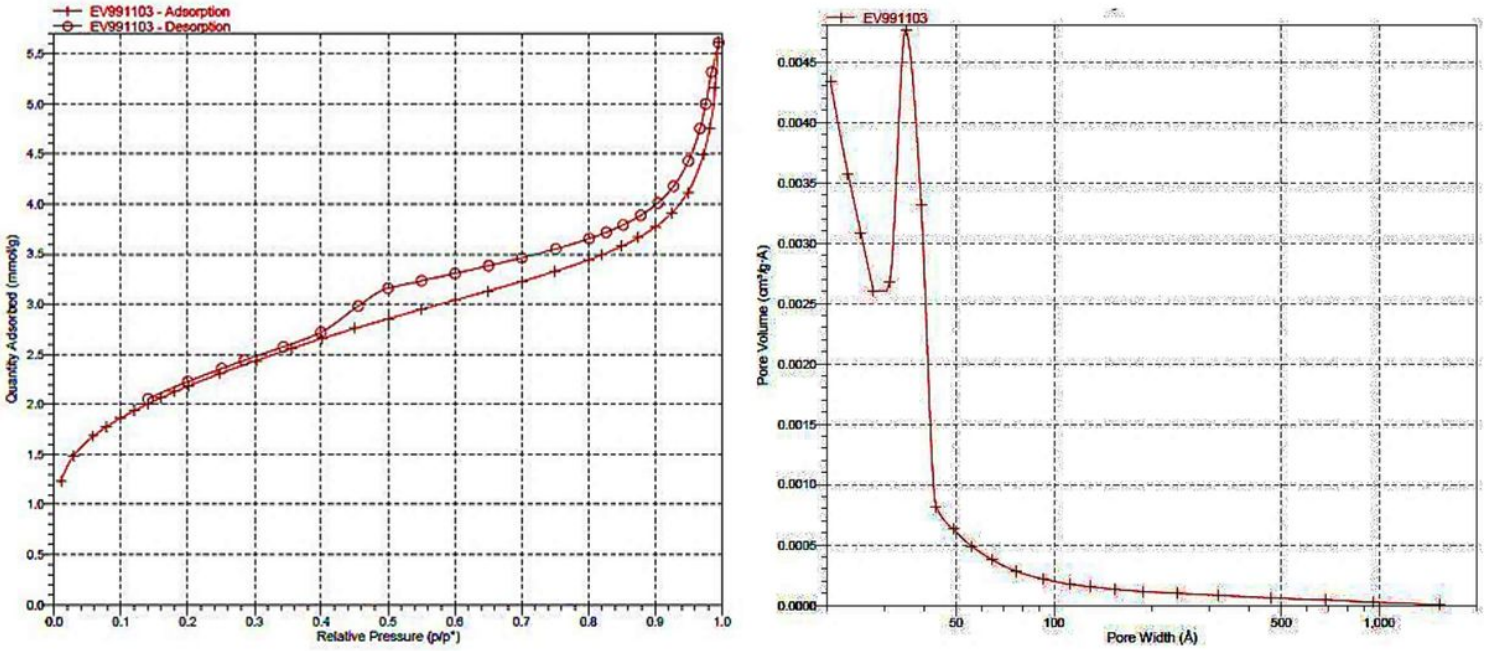

Figure 6

Adsorption/desorption isotherm of the Cu@APS-TDU-PMO (**1**).

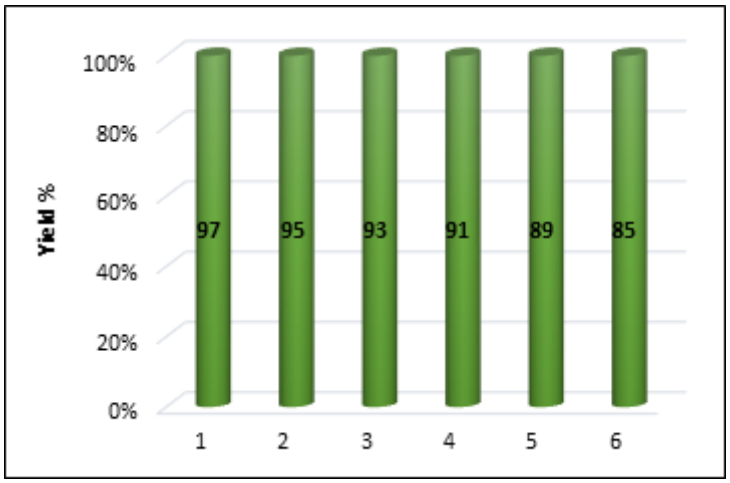

Figure 7

Reuse of the heterogeneous catalyst Cu@APS-TDU-PMO (**1**) for the synthesis of **5a.**

Supplementary Files

This is a list of supplementary files associated with this preprint. Click to download.

- Scheme01.png
- Scheme02.png
- Scheme03.png
- SupportingInformation3.docx